

# An Incrementally Deployed Swarm of MAVs for Localization Using Ultra-Wideband

Dominik Natter

Klaus Ening<sup>†</sup>

Claudio Paliotta

**Abstract**—Knowing the position of a moving target can be crucial, for example when localizing a first responder in an emergency scenario. In recent years, ultra wideband (UWB) has gained a lot of attention due to its localization accuracy. Unfortunately, UWB solutions often demand a manual setup in advance. This is tedious at best and not possible at all in environments with access restrictions (e.g., collapsed buildings). Thus, we propose a solution combining UWB with micro air vehicles (MAVs) to allow for UWB localization in a priori inaccessible environments. More precisely, MAVs equipped with UWB sensors are deployed incrementally into the environment. They localize themselves based on previously deployed MAVs and on-board odometry, before they land and enhance the UWB mesh network themselves. We tested this solution in a lab environment using a motion capture system for ground truth. Four MAVs were deployed as anchors and a fifth MAV was localized for over 80 second at a root mean square (RMS) of 0.206 m averaged over five experiments. For comparison, a setup with ideal anchor position knowledge came with 20% lower RMS, and a setup purely based on odometry with 81% higher RMS. The absolute scale of the error with the proposed approach is expected to be low enough for applications envisioned within the scope of this paper (e.g., the localization of a first responder) and thus considered a step towards flexible and accurate localization in a priori inaccessible, GNSS-denied environments.

## I. INTRODUCTION

The localization of a moving target is an often desired task. In search and rescue (SAR) missions knowing the position of a first responder can save that person's life in case of an accident. Autonomous sampling of seabeds, which can be useful for assessing environmental impacts, demands accurate positioning of an unmanned underwater vehicle. Similarly, on planetary missions the tracking of rovers or astronauts can be beneficial during exploration [1]. Often, localization strategies rely on external references like a global navigation satellite system (GNSS). However, in the aforementioned environments (indoors, underwater, or in outer space) GNSS is not available. In addition, these environments are challenging because they a) are not accessible a priori (i.e., no on-site preparations can be conducted in advance) and b) are often medium to large scale.

Various alternatives to GNSS have been proposed for localization of moving targets. In fact, the number of different

The INGENIOUS project has received funding from the European Union's Horizon 2020 Research and Innovation Programme and the Korean Government under Grant Agreement No 833435. Content reflects only the authors' view and the Research Executive Agency (REA) and the European Commission are not responsible for any use that may be made of the information it contains.

All authors are with SINTEF Digital, Trondheim, Norway.

{firstname.lastname}@sintef.no

<sup>†</sup>Corresponding Author



Fig. 1. An incrementally deployed swarm of four MAVs is used to localize a fifth MAV. The figure depicts three phases: a) the pre-deployment phase, b) the incremental deployment phase, and c) the localization phase with the localized MAV encircled in red. The base station is located on the left hand-side outside the captured images.

technologies is large and has led to several surveys (see, e.g., [2], [3]). Thus, a full overview is out of scope for this work. Instead, we focus on technologies we deem relevant to the scope of the proposed solution. We look at two types of alternatives to GNSS: some are external referencing systems (just like GNSS) whereas others run solely on the moving target.

Starting with the latter, solutions based on on-board sensors like accelerometers, gyroscopes, or magnetometers have been available for decades [4]. However, such dead reckoning systems drift over time, leading to intolerable errors in longer operations [5]. In recent years, the usage of more complex sensors like cameras or lidars for localization has received a lot of interest. Approaches like visual odometry (VO) or simultaneous localization and mapping (SLAM) allow to determine the object's position by exploiting sequential sensor measurements. Nowadays, such algorithms are available open-source, easily deployable, and achieve good localization accuracy (see, e.g., [6], [7]). Despite all recent improvements, these approaches still face some problems. Amongst others, the algorithms can be too computationally expensive for constrained devices, require extensive parameter tuning, and assume a static environment. Thus, large-scale environments can pose a problem [8].

When referring to external referencing systems, often so-called motion capture systems are used. These rely on

a set of well calibrated cameras to track markers within their common field of view. Such solutions score with high measurement frequencies and high accuracy [9]. However, due to the required initial setup and calibration these are not viable for use in the aforementioned environments.

Instead of using cameras, other external solutions rely on acoustic, magnetic, or different electromagnetic signals. The ad-hoc deployment of such systems has been shown previously [10], which makes them useful for a priori inaccessible environments. In addition to positioning, the decentralized fashion of such systems inherently allows for communication as well [11]. This allows to transmit the current location to a ground station outside the environment, which can be useful for live data reporting amongst others. The achievable accuracy and coverage, respectively, vary based on the underlying physical principles and thus can be tailored to the requirements of the desired environments [3].

Based on the analysis conducted in the preceding paragraphs we decide to rely on one of these external referencing systems. Of those, we choose ultra wideband (UWB) technology because it has received wide attention in recent years. Its reputation stems from various positive properties such as its high accuracy and the possibility to pass through obstacles [2].

A UWB setup for localization usually consists of multiple modules fixed in the environment (in the following referred to as anchors), which allow to determine the position of one or multiple moving modules (in the following referred to as tags). For this principle to work, the anchor positions must be known in advance. This often goes hand in hand with a tedious manual setup [12].

To avoid this step, we forge a bridge to another uprising technology: micro air vehicles (MAVs). Such miniaturized aircraft come in various designs. Of those, quadrotors are especially popular due to their maneuverability and vertical takeoffs amongst others [13]. The small size entails additional benefits such as increased safety and reduced costs. The latter allows MAVs to be used in large quantities to cover large environments (see, e.g., [14]). Even though small size comes with limited capabilities, recent progress allows for complex on-board calculations such as deep neural networks [15].

This paper builds upon the recent improvements in both UWB and MAV technology to localize targets in a priori inaccessible, GNSS-denied environments of variable size. In the proposed approach, MAVs fly into the environment relying on both on-board sensors and previously deployed MAVs for positioning. After landing the MAVs then function as UWB anchors for both subsequent MAVs / anchors and any UWB tag to be localized. Such *incremental* deployment removes the need for an initial setup and thus allows the system to enter a priori inaccessible environments. In addition, it makes the solution scalable to environments of various sizes. In order to function in the real world, such an approach needs to overcome many challenges. As a first step in that direction, this initial study focuses on assessing the localization performance of such an approach under some easing assumptions.

Thus, a large part of this work revolves around experimental results collected in a lab environment as shown in Figure 1. To the best of our knowledge this is the first publication experimentally showcasing such behavior. This quantitative analysis as well as more exhaustive information on related work and the technical implementation extends our previous work [16], where mostly the basic concept was presented.

## II. RELATED WORK

Similar concepts have been proposed in recent years.

Howard et al. presented a seminal work about incrementally deployed robot swarms [17]. They provide conceptual algorithms and detailed studies on coverage and scalability for their concept. However, their results are limited to a simulation study and each anchor is assumed to have ideal positioning knowledge.

A similar concept for incremental deployment of robots was proposed by Stirling et al. [18], [19]. Their first paper [18] includes algorithms and simulation studies, the follow-up paper [19] demonstrates experimental results with unmanned aerial vehicles (UAVs). The UAVs with a diameter of 550 mm and a weight of 600 g use a 3D infrared sensor to estimate their ego-motion based on other UAVs in the environment. However, at any point in time a flying UAV relies only on one other UAV, which can potentially lead to reduced robustness and localization accuracy compared to solutions relying on multiple deployed UAVs. In addition, their experiment was limited to only one flying UAV with the other anchors manually placed before the experiment, hence showcasing only a very limited form of incremental deployment.

An approach for 3D localization in mines using magneto-inductive sensors is found in [20]. One single calibrated sensor allows to initialize / localize deployed anchors, which then can be used to localize tags. More anchors can be added over time, which makes the solution scalable. However, the automatic deployment of these anchors is not addressed.

A concept with mobile anchors in underwater environments has been proposed as well [21]. In that work, the anchors regularly surface to get GPS signal and then dive down to localize a tag. This is conceptually similar to the proposed paper given that the anchors get an initial pose estimate, then move based on ego-motion, and finally localize a tag afterwards. However, the anchors are not used for supporting the state estimates of other anchors. In addition, the behavior was only analyzed in simulation.

Different authors have proposed and implemented solutions where a tag is localized by a set of anchors mounted on a mobile unit (see, e.g., [22]–[24]). The mobility of the anchor platform allows for deployment in a priori inaccessible environments. However, these concepts do not show any incremental behavior. In addition, placing all anchors on the same platform limits the possible localization coverage, which is especially crucial if multiple tags shall be localized.

Overall, different concepts for localization in a priori inaccessible, GNSS-denied environments have been proposed before. However, they often stop with simulation studies. In

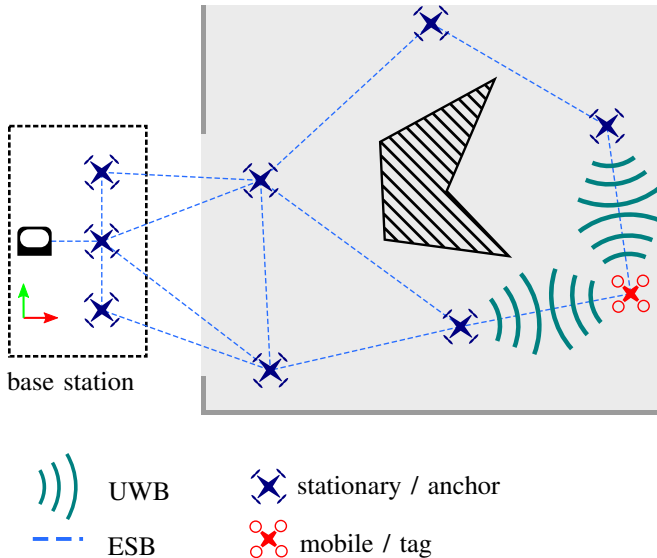


Fig. 2. The setup used in this paper is shown during the incremental deployment phase. On the left-hand side lies the base station consisting of a laptop and three MAVs (enclosed in dashed black). On the right-hand side lies an a priori inaccessible environment (rectangular area highlighted in grey). Five MAVs have already been deployed and remain stationary on the floor (dark blue). A sixth MAV (red) is currently traversing the environment, supported by two MAVs via UWB (green waves). Information like the position of the flying MAV can be relayed to the base station via our communication protocol based on ESB (dashed blue).

addition, the presented experimental results are either limited in size or do not showcase incremental and / or automatic deployment of anchors. Finally, no concept relies on MAVs and combines them with UWB technology. Thus, we regard this paper as an extension of the state of the art given its experimental validation of an incrementally deployed swarm of MAVs for localization using UWB.

### III. METHODS

In this section we explain the details of both the proposed concept and the technical implementation.

#### A. Concept

The goal is to achieve localization of a moving target in GNSS-denied, a priori inaccessible environments of variable size. In a UWB setup a set of anchors gets installed first, before a target can be localized by them. In a conventional setting this initial procedure demands manual labor of a human to first place the anchors in the environment and then measure their positions with respect to a common coordinate system. By contrast, our solution gets rid of this initial manual installation, making the system more flexible and drastically reducing the humans' workload. To do so, the UWB modules are deployed into the field on moving platforms. While MAVs are our platforms of choice, the concept can be applied to other platforms like unmanned ground vehicles. These MAVs disperse in the environment, land, and then serve as anchors. The internal state estimate of the MAV is used as the anchor's position, removing the need for manual measurements.

While the deployment of all MAVs could happen simultaneously, we propose to deploy them in an incremental fashion instead. The idea of such an incremental deployment is depicted in Figure 2. The MAVs enter the environment one after the other. Any flying MAV (like the one in red in Figure 2) relies on both odometry and landed MAVs (depicted in dark blue in Figure 2) for localization. Consequentially, after landing an MAV will support subsequent flying MAVs. Later, any moving target equipped with a UWB tag can take the place of the flying MAVs and thus be localized by the incrementally deployed anchors. Such incremental deployment comes with two distinct benefits compared to deploying all MAVs at once: For one thing, it increases the positioning accuracy of all anchors compared to using only odometry, as any flying MAV can rely on previously deployed anchors during flight. For another thing, it allows to flexibly enhance the UWB mesh network in later stages of the operation. As an additional benefit of our solution, the created mesh network allows to communicate the target's position to a base station outside of the environment (as on the left-hand side of Figure 2). This benefit is exploited in the proposed approach as explained in Section III-B.

#### B. Technical Implementation

With the general concept being elaborated, this section deals with its technical implementation.

**UWB Modalities:** In Section I, UWB has been identified as the most suitable technology for localization. When using UWB, different methods for localization exist. These include angle of arrival (AoA), received signal strength (RSS), time difference of arrival (TDoA), and time of arrival (ToA) (see, e.g., [25]). In the following some pros and cons are listed. AoA has an acceptable accuracy, but is complex to implement and maintain [2]. RSS is not very accurate, especially at large distances [25]. This might partly be because it does not exploit the high bandwidth inherent in UWB well [2]. TDoA conventionally demands a clock sync between all anchors [25]. On the other hand, no synchronization is needed between the tag(s) and the anchor(s). Thus, TDoA scales well with the number of tags [26]. For ToA no synchronized anchors are needed, while it often demands a synchronization between the tag and the anchor. However, this can be avoided with certain protocols, such as two-way ranging (TWR) [25]. ToA allows to achieve higher accuracy than TDoA [2]. In addition, the performance degradation outside the anchor's convex hull is lower for ToA than for TDoA [26]. This is highly relevant for our concept, where MAVs regularly must leave the convex hull to expand the mesh network. Based on this analysis, we choose a TWR implementation of ToA.

**MAV Platform:** For the moving platforms we choose MAVs due to their advantages described in Section I. In theory, however, the proposed concept can be adapted to other platforms like unmanned ground vehicles. After scanning the market we chose the Crazyflie 2.1 from Bitcraze AB<sup>1</sup>, a

<sup>1</sup><https://www.bitcraze.io/products/crazyflie-2-1/>

product widely spread in different research communities<sup>2</sup>. With its diameter of 130 mm and its weight of less than 40 g we consider it an MAV. The Crazyflie is a modular platform, which allows to add different sensors on so-called decks. In addition to the on-board IMU, we have added an optical flow deck (incl. a 1D lidar) for velocity and altitude estimation, as well as a UWB deck. The UWB deck includes a Decawave DWM1000 module, which Bitcraze tested at up to 10 m range. All available sensor measurements are fused in an extended Kalman filter [27], [28]. This permits to use odometry when UWB signals are not available and a combination of odometry and absolute positioning when UWB signals are available. Thus, this platform is a suitable choice to showcase the proposed concept.

All MAVs use the same hardware and software, which is helpful for scaling the solution to large swarms. In addition, the firmware is available open source, which facilitates the development and future re-usage through the research community. For this project, only some minor adaptations have been performed on this firmware. These are needed to allow the MAVs to switch their UWB behavior: while flying a MAV should localize itself with respect to previously deployed MAVs (i.e., act as a tag), whereas after landing it should provide localization to subsequent MAVs (i.e., act as an anchor).

**Base Station:** In order to provide the first MAV with good absolute localization without previously deployed MAVs, a pre-calibrated base station with three MAVs in known positions is used (this is depicted in the left part of Figure 2). As of now, this base station must be placed in an a priori *accessible* environment. In future experiments, the base station could be a mobile unit itself (similar to [22]). If placed within reach of a GNSS the base station can provide the whole mesh network with a global reference.

**Swarm Communication Protocol:** To control the swarm and read out information an inter-MAV communication is set up. Next to UWB signaling, the MAVs allow for wireless communication via an on-board nRF51822 chip and Nordic Semiconductor’s Enhanced ShockBurst (ESB) protocol. This protocol is exploited to exchange messages between nearby MAVs (as indicated in dashed blue in 2). By relaying, such messages information can traverse through the whole swarm. The main goal of such relaying is to communicate with a user outside the environment. Exemplarily, this allows a user to read out the current position of the moving target, check the battery status of landed MAVs, or tell the next MAV where to go. To implement such behavior each MAV is assigned an ID upon start-up. The communication strategy is based on broadcasting and for simplicity reduced to two modes: A message is either broadcast to all neighbors (i.e., MAVs within communication range), or the whole swarm. Based on the ID included in a message header any MAV decides to react to, relay or acknowledge this message. This concept works inherently within the swarm without additional equipment. However, if desired, an operator can

be involved via a laptop. In order to bridge the laptop and the swarm we connect the laptop to one MAV via ESB or USB. This MAV, specified via its ID, serves as the connection between the swarm and the laptop in both directions. The user interface on the laptop is written in Python, whereas the firmware on the MAVs is written in C. Messages are transformed following pre-defined type definitions. We want to stress again that the communication protocol works independently. Thus, in the future the complete swarm logic can be implemented on-board of the individual MAVs, rendering the connected laptop optional and for centralized information only.

#### IV. EXPERIMENTAL SETUP

In order to test the proposed concept, an experiment in an office environment is conducted. The environment spans approx.  $7\text{ m} \times 5\text{ m}$  and is covered by a Qualisys motion capture system.

**Base Station:** Adjacent to this environment the base station is set up. This consists of a laptop, a MAV connected to the laptop via USB, and two Loco Positioning nodes. A Loco Positioning node is another product from Bitcraze<sup>3</sup>. Most commonly, it is used as a UWB anchor for the localization of the MAVs. It contains the same UWB chip and uses the same firmware as the MAVs, but comes at reduced cost due to other savings (e.g., no motors being attached). Previously conducted in-house tests suggest that the localization performance is the same, irrespective of whether MAVs or Loco Positioning nodes are used as anchors. Thus, we are confident that replacing two MAVs of the base station by two Loco Positioning nodes does not affect our experiments. The three anchors are set up in a line spanning 1.9 m, with the two outer anchors at 0.15 m and the middle anchor at 1.1 m above the floor, respectively.

**Incremental Deployment:** Using the base station, four MAVs are deployed incrementally. This means that every MAV relies on both the three ground station anchors and all previously deployed MAVs for localization. The takeoff of each MAV happens upon a dedicated user input via the designed Python interface. Each MAV flies into the center of the environment, rotates, and flies to a separate corner of a pre-determined square (approx.  $2.8\text{ m} \times 2.8\text{ m}$ ). Reaching its final position it lands and turns into a UWB anchor. The final mesh network thus consists of five MAVs and two Loco Positioning nodes.

Next, another MAV is deployed as an example of a moving target. After takeoff, it flies four laps on a pre-determined rectangle ( $4\text{ m} \times 2\text{ m}$ ), thus traveling 48 m. Then it lands without switching to anchor mode. We refer to such a flight as an evaluation flight. For the given mesh network, the same MAV performs three of these evaluation flights, with the settings differing as follows:

- 1) In the first case, the approach proposed in this paper is used: deployed MAVs use their state estimates to aid the localization of subsequent MAVs via UWB. Hence

<sup>2</sup><https://www.bitcraze.io/portals/research/>

<sup>3</sup><https://www.bitcraze.io/products/loco-positioning-node/>

this case is referred to as *our approach* in the following sections.

- 2) In the second case, the positions of the deployed MAVs are updated with ground truth values retrieved from the motion capture system. This allows us to showcase a scenario with perfectly known anchor positions as one could ideally achieve them with a prior, manual setup procedure. Thus, this case is denoted as *ideal anchors*.
- 3) In the last case, the UWB deck is removed from the flying MAV. This allows us to analyze the performance of the on-board odometry in an isolated manner. Accordingly, this case is called *no anchors*.

The whole procedure (i.e., mesh network creation and three evaluation flights) is repeated 5 times for statistical significance. In each repetition the same MAVs are used. All MAVs fly at an altitude of 1 m with a maximum speed of  $1 \text{ m s}^{-1}$ . The motion capture system records all the flight trajectories and is used to update the deployed MAV positions in the *ideal anchors* case, but it is never fused into the state estimator of a *flying* MAV.

**Logging:** Different data is logged for analysis of the experiments. In order to log the motion capture values the data is streamed to the base station via TCP at a rate of 10 Hz. Similarly, the state estimates of the flying MAV are streamed to the base station using Bitcraze’s logging functionality at a rate of 10 Hz. The anchor positions are relayed through the swarm communication at a rate of approx. 1 Hz. In all three cases, the data is first combined with the current timestamp of the base station and then written to a csv file.

**Metrics:** We want to assess both the localization of flying targets as well as the accuracy of anchor positions. In order to do so, an error between the ground truth values and the state estimates is introduced in the form of

$${}^j_i \mathbf{e}_k = [{}^j_i e_{x,k} \quad {}^j_i e_{y,k} \quad {}^j_i e_{z,k}]^T = {}^j_i \mathbf{p}_{g,k} - {}^j_i \hat{\mathbf{p}}_k, \quad (1)$$

where  $\mathbf{e}$  are the errors,  $\mathbf{p}_g$  are the ground truth values, and  $\hat{\mathbf{p}}$  are the state estimates. All vectors contain three values for the three spatial axes ( $x$ ,  $y$ , and  $z$ ). Furthermore, the indices denote the following:

- $i$  can stand for two different values:
  - $i \in \{1, \dots, 4\}$  denotes the four deployed MAVs when analyzing the anchor positions.
  - $i \in \{\textit{our approach}, \textit{ideal anchors}, \textit{no anchors}\}$  denotes the three settings when analyzing the evaluation flights.
- $j \in \{1, \dots, 5\}$  denotes the five repetitions.
- $k$  denotes the time. For the anchor analysis  $k$  is a fixed timestamp after landing, whereas for the evaluation flights  $k$  is an index indicating the progress between takeoff and landing. The timestamps for takeoff and landing are extracted automatically based on the MAV’s altitude and a threshold of 0.1 m.

These error values are then used in different metrics. For the anchor analysis, the Euclidean distance is calculated for all deployed anchors and all repetitions. Then we report the

TABLE I  
3D EUCLIDEAN ERRORS FOR THE FOUR DEPLOYED MAVS AFTER LANDING. HIGHER ID INDICATES LATER DEPLOYMENT. BOTH AVERAGE AND STANDARD DEVIATION (SD) ARE CALCULATED OVER ALL 5 EXPERIMENTS.

ID	Average [m]	SD [m]
1	0.097	0.040
2	0.134	0.049
3	0.200	0.036
4	0.153	0.031

average and standard deviation of these Euclidean distances over the repetitions. For the evaluation flights two metrics are of interest:

- A component-wise average and standard deviation over the five experiments are calculated to analyze the performance over flight time.
- The root mean square (RMS) of the Euclidean distance is calculated for each setting and each repetition, in order to quantify entire flights at once.

## V. RESULTS

Based on the explanations given in the preceding paragraphs, the results are presented next.

Starting with the mesh network creation, Table I lists the statistical variation of the anchor positioning errors, i.e., the differences between the on-board estimated positions of the deployed MAVs after landing and the ground truth positions measured by the motion capture system. The average errors vary between approx. 0.1 m and 0.2 m, with standard deviations on the order of 0.04 m.

Moving on to the evaluation flights, Figure 3 depicts the flight paths of all evaluation flights as measured by the motion capture system. The flights are distinguished by color based on the chosen setting. The plot indicates that flights in the *ideal anchors* case come with less variation than flights in the *our approach* case. Furthermore, both lead to consistent absolute positioning over time, which is not true for flights in the *no anchors* case. Overall, the flying MAV traveled approximately 720 m.

Figure 4 allows to take a closer look at the performance in each of the three cases. Here the errors between position estimates and motion capture measurements are plotted over time. The times between takeoff and landing are chosen as the interval on the  $x$ -axis. These vary between approx. 80 s and 90 s among all flights. For a statistical representation of the five experiments performed for each setting, the averages and standard deviations over these five experiments are depicted. The errors in the  $z$ -axis are lowest for all settings, varying in the range of a few centimeters only. The errors in the horizontal axes are larger than in the  $z$ -axis, with errors in both the  $x$ - and the  $y$ -axis being on similar levels. As already indicated in Figure 3, the *no UWB* case features the highest average errors. In addition, a drifting behavior can be seen both by the increasing average in the  $x$ -axis and the increasing standard deviation in the  $y$ -axis. Both *our approach* and *ideal UWB* do not show such drifting behavior

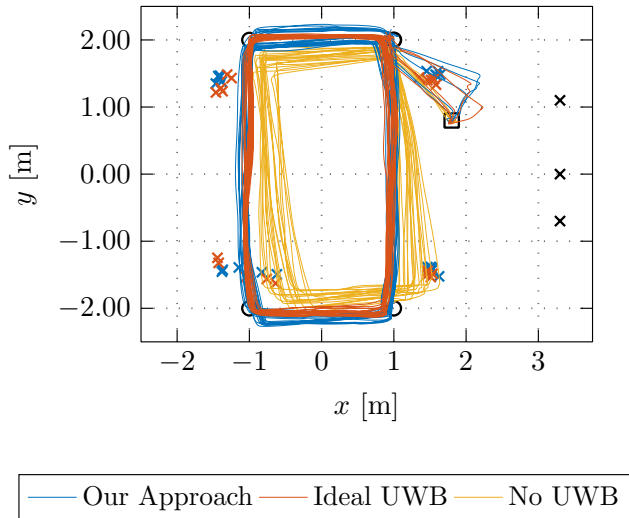


Fig. 3. A bird's-eye view of the flight paths of all evaluation flights as measured by the motion capture system. The paths are colored by the setting used. For each setting five experiments with four laps and thus 20 rectangles in total are plotted. The black square indicates the starting position of the flying MAV and the four black circles indicate the setpoints commanded to this MAV. The crosses denote the anchors: black is for the base station anchors, blue for deployed anchors reporting state estimates, and red for deployed anchors reporting ideal ground truth values. For each of the five experiment four MAVs are deployed as anchors, resulting in 20 blue and 20 red crosses. This figure is best viewed in color.

and come with lower errors. While the average errors are similar among those two, *our approach* comes with higher standard deviations.

The errors depicted over time in Figure 4 are quantified in Figure 5 by means of RMS values. The *ideal UWB* case comes with the lowest RMS values, varying between 0.121 m and 0.2 m with a mean value of 0.159 m over the five experiments. *Our approach* shows a comparable performance with RMS values ranging from 0.123 m to 0.268 m with a mean value of 0.202 m. The *no anchors* case exhibits the highest RMS values, ranging from 0.303 m to 0.491 m with a mean value of 0.371 m.

## VI. DISCUSSION

Looking at the results discussed in the previous section, a few points specifically draw our attention.

### A. Target Localization

On average the proposed approach shows a 27% increased RMS compared to the *ideal anchor* case. Additionally, the proposed approach comes with an increased variation in positioning accuracy. Still, in some experiments the performance of *our approach* is on par with or even better than in the *ideal UWB* case. To contextualize the results multiple aspects have to be considered. First, the overall reduction in accuracy has to be weighed up against the advantages of the proposed approach (no labor-intensive setup needed, useful in a priori inaccessible environments). Furthermore, the absolute accuracy requirements vary based on the specific application. With potential applications mentioned in Section I in mind (e.g., localization of a first responder), the achieved

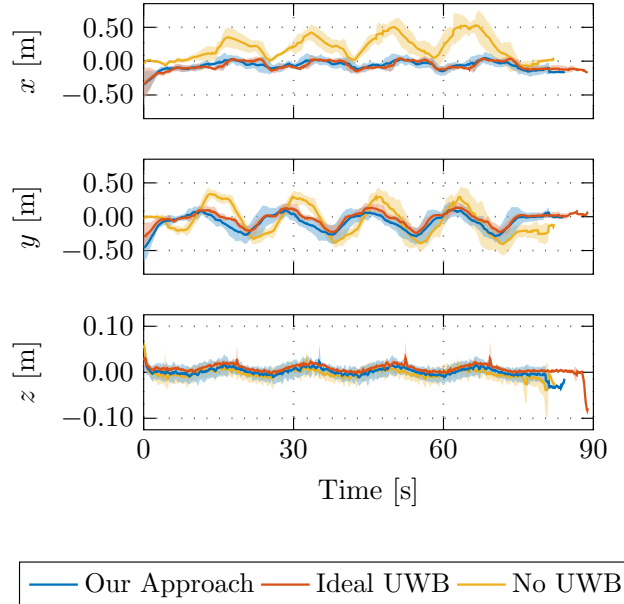


Fig. 4. Error values of the flying MAV over time, split in the x-, y-, and z-direction, respectively. The lines are colored by the setting used. For each setting the average (thick line) and standard deviation (semi-transparent shadow) are calculated over five experiments. Errors are calculated between takeoff and landing. Due to varying flight durations the shown statistics do not necessarily include all five flights for time values above 80 seconds. This figure is best viewed in color.

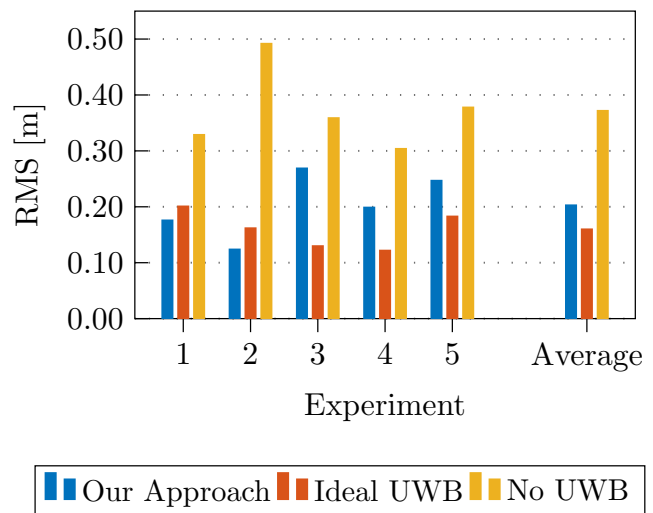


Fig. 5. RMS values of the 3D Euclidean Errors for all evaluation flights. The values are shown for the different settings (colors) and over all five experiments (horizontal axis). In addition, the averages of the five previous RMS values for each setting are plotted on the right. This figure is best viewed in color.

accuracy of the proposed approach can be deemed high enough.

As indicated in Section I and underlined by the performance of the *no UWB* case (84% higher average RMS value compared to *our approach*), odometry alone is not enough for accurate long-term localization. However, the drift seems to happen rather slow (maximum 3D Euclidean errors are below 1 m compared to the traveled distance of almost 50 m). This can be beneficial for the mesh network creation phase. In order to build up a mesh network, each individual MAV must go beyond the convex hull of the mesh network before it lands. In this period outside the convex hull, UWB localization performance is degraded [26]. This effect is more pronounced for sparser mesh networks, as MAVs must fly further beyond the mesh network boundaries. Thus, this justifies our choice of relying on a combination of UWB and odometry for building an accurate mesh network: with odometry alone creating a *large* mesh network is difficult, while UWB alone struggles to create a *sparse* (and thus cost-efficient) mesh network.

In all three cases, the errors in the z-axis are substantially lower than in the x- and y-axis. This is due to the 1D lidar mounted on the MAVs, which provides an additional absolute measurement in this axis. In contrast, in the x- and y-axis UWB measurements are the only absolute measurements.

Comparing the results with existing work helps to further contextualize them. All the works discussed in Section II differ from the proposed approach to a certain degree, making detailed statements difficult. Under those limitations, the work presented in [19] is chosen as a baseline, as it is closest both to the proposed concept (i.e., incremental deployment of aerial vehicles for localization) and includes the most advanced physically conducted experiments. Different quantitative values for both papers are collected in Table II. The vehicles used in [19] come with an approx. four times larger diameter and 20 times higher weight compared to the MAVs used in this paper. In addition to odometry they rely on an infrared sensor for localization, compared to UWB proposed in this paper. In their experiments two anchors were placed in the environment manually (i.e., without prior incremental deployment). Then one flying vehicle was deployed. For localization, this vehicle relied on a maximum of one anchor at a time. In comparison, in this paper we deploy five vehicles, where each relies on all previously deployed vehicles and the three anchors of the base station. For the evaluation flights this equals seven different UWB signals used for localization. The experiments conducted in [19] included only flights in a straight line along their *x*-axis. Thus, they provide results only for the two perpendicular axes. For these axes, they provide the total deviation from the straight line as measured by an external tracking system. In the *y*-axis they reported a mean position of  $-0.03$  m with a mean standard deviation (SD) of  $\pm 0.11$  m, in the *z*-axis a mean position of  $1.04$  m with a mean SD of  $\pm 0.16$  m, respectively. We use the errors

TABLE II  
DIFFERENT QUANTITIES FOR COMPARISON OF EXPERIMENTS  
CONDUCTED IN [19] AND IN THIS WORK.

Quantity	[19]	Ours
Vehicle Diameter [m]	0.55	0.13
Vehicle Weight [kg]	0.60	0.04
Number of Deployed Vehicles per Experiment	1	5
Max. Number of Anchors Used for Localization	1	7
Total Flight Distance [m]	120	720
Max. Flight Velocity [ $\text{m s}^{-1}$ ]	0.92	1.0

proposed in Eq. 1 for a rough comparison<sup>4</sup>. In *our approach*, the mean SDs for the *y*- and *z*-axis are 0.11 m and 0.017 m, respectively. Thus, the performance in the horizontal axes seem similar, while in the vertical axis the errors reported in this paper seem a magnitude lower. The maximum flight speeds were similar in both papers. This paper collected more flight data (more than 720 m for the evaluation flights in addition to 20 deployments of anchors, compared to 120 m in [19]). Overall, while acknowledging the quality of the work proposed by [19], we think that this paper enhances the state of the art set by them by using smaller vehicles, using a larger setup, and conducting more tests, while performing similarly or potentially even better in terms of navigation accuracy.

### B. Anchor Positioning

When looking at the achieved anchor accuracies, their values are in the range of the errors introduced by the biases inherent to the UWB modules itself [29]. One could expect that the errors reduce for later deployed MAVs (i.e., higher IDs in Table I), given that they have more anchors available to rely on. This is not the case in our experiments. We see three potential causes for this:

- 1) First, the scale of the experiment is small, leading to low distances travelled and thus low impact of odometry-induced drift.
- 2) Second, already the first deployed MAV can rely on three reference points at the base station, which supports its localization.
- 3) Third, the experimental setup demanded the MAVs to rotate before flying to the dedicated corner of the pre-determined rectangle. The rotation was lowest for the first MAV ( $45^\circ$ ) and highest for the fourth MAV ( $235^\circ$ ). It was observed by the operators that this rotation happened at high angular velocities, throwing the MAV off the track. This effect seemed more severe for larger rotations. The variance in landing positions of the fourth MAV as seen in Figure 3 supports this hypothesis.

<sup>4</sup>In our experiments, only four waypoints and thus no detailed reference trajectory are provided. Thus, no *direct* performance comparison is possible. However, the proposed errors between position estimates and motion capture measurements can provide at least a *rough* comparison based on this thought: If the controller of the MAV works ideally, the state estimates will be always on a straight line between the waypoints. In that case, the proposed error metric would align with the error metric in [19]. Indeed, an internal analysis of the collected data reveals that the MAV state estimates are close to such straight lines, allowing for a cautious comparison.

Overall, we expect varying anchor accuracies for tests at larger scale.

### C. Limitations

A UWB-related artifact can be seen in Figure 3: in both approaches relying on UWB the MAV used for evaluation at first moves *away* from the first setpoint sometimes. After exhaustive tests we relate this to degraded UWB accuracy when both anchor(s) and tag are on the floor and the distance surpasses certain levels (approx. 4m). The UWB-based distances are then overestimated, leading to the MAV estimating it is further away from the mesh network. This discrepancy between physical position and state estimate is also seen in the first few seconds of Figure 4. The effect vanishes as soon as the MAV has spent some time in the air. In real deployments the MAV will spend most of its time hovering above the mesh network, which is why no countermeasures were taken.

The conducted experiments come with two limitations, both caused by the use of the motion capture system: For one, the scale of the environment and thus the distances between landed MAVs are limited. A sparser mesh network and further travelled distances could potentially lead to different localization accuracies, which need to be investigated in more detail. For another, the tests were performed in an obstacle-free lab environment such that the motion capture system could track the MAVs at all times. We expect degraded UWB distance accuracies due to signal transmission delays when obstacles are blocking or reflecting the way of the signals.

In this work, the focus is on proposing an incrementally deployed swarm of MAVs and assessing its localization performance. Thus, the experiments are performed under certain favorable conditions such as the obstacle-free lab environment. We are aware that in a real-world use case, multiple complex challenges need to be overcome. For example, in a large-scale environment the operator will need a map to define the landing position for the MAV to be deployed next. In order to reach this landing position, the MAVs will have to traverse potentially complex environments with obstacles or dead ends. For this, obstacle avoidance and exploration capabilities are needed, keeping in mind the limited on-board sensing abilities of MAVs. This short example illustrates the scale of potential challenges to be faced on the way to robust real-world deployment. In this paper we assessed the localization performance of such a system and thus the general feasibility for more complex environments in the future.

Taking into account the aforementioned limitations, this paper has demonstrated the first implementation of an incrementally deployed swarm of MAVs. We consider this a successful demonstration, given that a target can be localized consistently over time with tolerable errors. This allows to move a step closer towards localization of objects in a priori inaccessible, GNSS-denied environments.

## VII. CONCLUSION

In this paper we have addressed the problem of localizing a target in a priori inaccessible, GNSS-denied environments. We have proposed a solution based on a mesh network of UWB anchors. Such anchors usually rely on a labor-intensive prior setup and thus access to the environment. In order to overcome this limitation, we use MAVs as UWB anchors. The state estimates of the MAVs are exploited as UWB anchor positions. To achieve this the state estimates from odometry sensors are enhanced by fusing UWB signals from previously deployed MAVs. To the best of our knowledge this is the first real-world implementation of such incrementally deployed swarm behavior using MAVs. To examine the performance tests were conducted in a lab environment with access to a motion capture system for ground truth. Four MAVs were deployed as anchors and a fifth MAV was localized for over 80 seconds at an RMS of 0.202 m averaged over five experiments. Compared to a setup with ideal anchor position knowledge this removes the need for both an initial labor-intensive setup and a priori access to the environment, at the cost of a 27% drop in localization (RMS value). A setup purely based on odometry comes with 84% higher RMS values compared to the proposed approach. The absolute scale of the error with the proposed approach is expected to be low enough to allow for applications envisioned within the scope of this paper (e.g., the localization of a first responder).

In future experiments we plan to test the localization accuracy in larger environments with tougher terrain and some obstacles or other disturbances. We further envision to improve the UWB-based localization with global optimization methods after deployment [29] and calibration of internal biases [26]. In addition, we intend to embed the solution in a more autonomous framework, allowing for smart deployment of MAVs based on maps and localization requirements.

## ACKNOWLEDGMENT

We want to thank Sigurd Mørkved Albrektsen for helpful input, especially his contributions to the UWB code, allowing MAVs to switch from tag to anchor mode.

## REFERENCES

- [1] S. Se, H.-K. Ng, P. Jasiobedzki, and T.-J. Moyung, "Vision based modeling and localization for planetary exploration rovers," in *55th International Astronautical Congress*, 2004.
- [2] A. Alarifi, A. Al-Salman, M. Alsaleh, A. Alnafessah, S. Al-Hadhrami, M. A. Al-Ammar, and H. S. Al-Khalifa, "Ultra wideband indoor positioning technologies: Analysis and recent advances," *Sensors*, vol. 16, no. 5, p. 707, 2016.
- [3] R. Mautz, "Indoor positioning technologies," Ph.D. dissertation, ETH Zürich, 2012.
- [4] B. Barshan and H. F. Durrant-Whyte, "Inertial navigation systems for mobile robots," *IEEE transactions on robotics and automation*, vol. 11, no. 3, pp. 328–342, 1995.
- [5] O. J. Woodman, "An introduction to inertial navigation," University of Cambridge, Computer Laboratory, Tech. Rep., 2007.
- [6] R. Mur-Artal and J. D. Tardós, "Orb-slam2: An open-source slam system for monocular, stereo, and rgb-d cameras," *IEEE transactions on robotics*, vol. 33, no. 5, pp. 1255–1262, 2017.

- [7] C. Forster, M. Pizzoli, and D. Scaramuzza, "Svo: Fast semi-direct monocular visual odometry," in *2014 IEEE international conference on robotics and automation (ICRA)*. IEEE, 2014, pp. 15–22.
- [8] C. Cadena, L. Carlone, H. Carrillo, Y. Latif, D. Scaramuzza, J. Neira, I. Reid, and J. J. Leonard, "Past, present, and future of simultaneous localization and mapping: Toward the robust-perception age," *IEEE Transactions on robotics*, vol. 32, no. 6, pp. 1309–1332, 2016.
- [9] P. Merriaux, Y. Dupuis, R. Boutteau, P. Vasseur, and X. Savatier, "A study of vicon system positioning performance," *Sensors*, vol. 17, no. 7, p. 1591, 2017.
- [10] P. Corke, C. Detweiler, M. Dunbabin, M. Hamilton, D. Rus, and I. Vasilescu, "Experiments with underwater robot localization and tracking," in *Proceedings 2007 IEEE International Conference on Robotics and Automation*. IEEE, 2007, pp. 4556–4561.
- [11] M. Ghavami and R. Kohno, *Ultra Wideband Signals and Systems in Communication Engineering*. John Wiley & Sons, 2004.
- [12] D. Lymberopoulos and J. Liu, "The microsoft indoor localization competition: Experiences and lessons learned," *IEEE Signal Processing Magazine*, vol. 34, no. 5, pp. 125–140, 2017.
- [13] M. Coppola, K. N. McGuire, C. De Wagter, and G. C. de Croon, "A survey on swarming with micro air vehicles: Fundamental challenges and constraints," *Frontiers in Robotics and AI*, vol. 7, p. 18, 2020.
- [14] B. P. Duisterhof, S. Li, J. Burgués, V. J. Reddi, and G. C. de Croon, "Sniffy bug: A fully autonomous swarm of gas-seeking nano quadcopters in cluttered environments," in *2021 IEEE/RSJ International Conference on Intelligent Robots and Systems (IROS)*. IEEE, 2021, pp. 9099–9106.
- [15] D. Palossi, N. Zimmerman, A. Burrello, F. Conti, H. Müller, L. M. Gambardella, L. Benini, A. Giusti, and J. Guzzi, "Fully onboard ai-powered human-drone pose estimation on ultra-low power autonomous flying nano-uavs," *IEEE Internet of Things Journal*, pp. 1913–1929, 2021.
- [16] C. Paliotta, K. Ening, and S. M. Albrektsen, "Micro indoor-drones (mins) for localization of first responders," *Proceedings of the 18th ISCRAM, Blacksburg, VA, USA*, 2021.
- [17] A. Howard, M. J. Matarić, and G. S. Sukhatme, "An incremental self-deployment algorithm for mobile sensor networks," *Autonomous Robots*, vol. 13, no. 2, pp. 113–126, 2002.
- [18] T. Stirling, S. Wischmann, and D. Floreano, "Energy-efficient indoor search by swarms of simulated flying robots without global information," *Swarm Intelligence*, vol. 4, no. 2, pp. 117–143, 2010.
- [19] T. Stirling, J. Roberts, J.-C. Zufferey, and D. Floreano, "Indoor navigation with a swarm of flying robots," in *2012 IEEE international conference on robotics and automation*. IEEE, 2012, pp. 4641–4647.
- [20] T. E. Abrudan, Z. Xiao, A. Markham, and N. Trigoni, "Underground incrementally deployed magneto-inductive 3-d positioning network," *IEEE Transactions on Geoscience and Remote Sensing*, vol. 54, no. 8, pp. 4376–4391, 2016.
- [21] M. Erol, L. F. Vieira, A. Caruso, F. Paparella, M. Gerla, and S. Oktug, "Multi stage underwater sensor localization using mobile beacons," in *2008 Second International Conference on Sensor Technologies and Applications (sensorcomm 2008)*. IEEE, 2008, pp. 710–714.
- [22] K. C. Cheok, M. Radovnikovich, P. Vempaty, G. R. Hudas, J. L. Overholt, and P. Fleck, "Uwb tracking of mobile robots," in *21st Annual IEEE International Symposium on Personal, Indoor and Mobile Radio Communications*. IEEE, 2010, pp. 2615–2620.
- [23] A. Wallar, B. Araki, R. Chang, J. Alonso-Mora, and D. Rus, "Foresight: Remote sensing for autonomous vehicles using a small unmanned aerial vehicle," in *Field and Service Robotics*. Springer, 2018, pp. 591–604.
- [24] S. Güler, M. Abdelkader, and J. S. Shamma, "Peer-to-peer relative localization of aerial robots with ultrawideband sensors," *IEEE Transactions on Control Systems Technology*, 2020.
- [25] Z. Sahinoglu, S. Gezici, and I. Guvenc, "Ultra-wideband positioning systems," *Cambridge, New York*, 2008.
- [26] W. Zhao, J. Panerati, and A. P. Schoellig, "Learning-based bias correction for time difference of arrival ultra-wideband localization of resource-constrained mobile robots," *IEEE Robotics and Automation Letters*, vol. 6, no. 2, pp. 3639–3646, 2021.
- [27] M. W. Mueller, M. Hamer, and R. D'Andrea, "Fusing ultra-wideband range measurements with accelerometers and rate gyroscopes for quadcopter state estimation," in *2015 IEEE International Conference on Robotics and Automation (ICRA)*, May 2015, pp. 1730–1736.
- [28] M. W. Mueller, M. Hehn, and R. D'Andrea, "Covariance correction step for kalman filtering with an attitude," *Journal of Guidance, Control, and Dynamics*, pp. 1–7, 2016.
- [29] M. Hamer and R. D'Andrea, "Self-calibrating ultra-wideband network supporting multi-robot localization," *IEEE Access*, vol. 6, pp. 22 292–22 304, 2018.